ELSEVIER

Journal of Fluids and Structures 26 (2010) 1142–1154

JOURNAL OF FLUIDS AND STRUCTURES

www.elsevier.com/locate/jfs

Experimental study on wind loading on a complicated group-tower

Ming Gu[a,*], Peng Huang[a], Lin Tao[a], Xuanyi Zhou[a], Zhong Fan[b]

[a]*State Key Laboratory of Disaster Reduction in Civil Engineering, Tongji University, Shanghai 200092, China*
[b]*China Architecture Design and Research Group, Beijing 100044, China*

Received 21 July 2009; accepted 21 August 2010
Available online 20 October 2010

Abstract

This paper studied how wind pressures and forces affect rigid sectional models of a complicated group-tower using experimental wind tunnel tests. The group-tower was composed of five separate sub-towers with different diameters and heights. The basic characteristics of the mean and fluctuating wind pressure distributions on typical parts of the sub-towers were analyzed along the heights of each sub-tower, and their distribution trends are discussed. Also, the mean base shear and moment coefficients and their characteristics are presented. The wind pressure and wind force results showed that because the group-tower structure consisted of five separate lofty towers, the mutual aerodynamic interferences were serious; thus, the mean and fluctuating wind pressure, wind force distributions and the mean base shear and moment coefficients were quite complicated.

Keywords: Group-tower; Sub-tower; Wind tunnel test; Interference effect; Wind pressure; Wind force

1. Introduction

Wind loading is a dominant force acting on lofty tower designs. Many studies on wind loading and its effect on high-rise structures have been done (Katsumuraa et al., 2001; Breuera and Chmielewskib, 2002; Gu and Quan, 2004; Kim and You, 2002; Mahon and Meskell, 2009) in which interference effects among high rise towers and tall buildings were discussed (Masaaki, 1998; Xie and Gu, 2004, 2007). In one study, Xie and Gu (2004) used wind tunnel tests to deduce a simple formula that estimates the interference factors among three tall buildings. Gu and Sun (1999, 2001) studied the interference effect between two and three circular cylinders in uniform, smooth flows and found that the spacing ratios (the ratio of the distance between the cylinders to the diameter of the cylinders) had a great influence on the aerodynamic force coefficients of the cylinders. Sun and Gu (1995) also found that when four towers were arranged in a rhomboid, the peak suctions on the two downstream cooling towers were larger than that of an isolated tower. Li and Sumner (2009) conducted wind tunnel experiments to measure the vortex shedding frequencies for two circular cylinders of finite height arranged in a staggered configuration with closely, moderately and widely spaced configurations. It was found that the Strouhal numbers and flow patterns change along the cylinder. In addition to wind tunnel experimental methods, CFD techniques have been used to study wind pressure and force distributions acting on group-tower system. Lam et al. (2008) made two- and three-dimensional numerical simulations of cross-flow around

*Corresponding author. Tel.: +86 21 65982893; fax: +86 21 65458965.
E-mail address: minggu@tongji.edu.cn (M. Gu).

0889-9746/$ - see front matter © 2010 Elsevier Ltd. All rights reserved.
doi:10.1016/j.jfluidstructs.2010.08.003

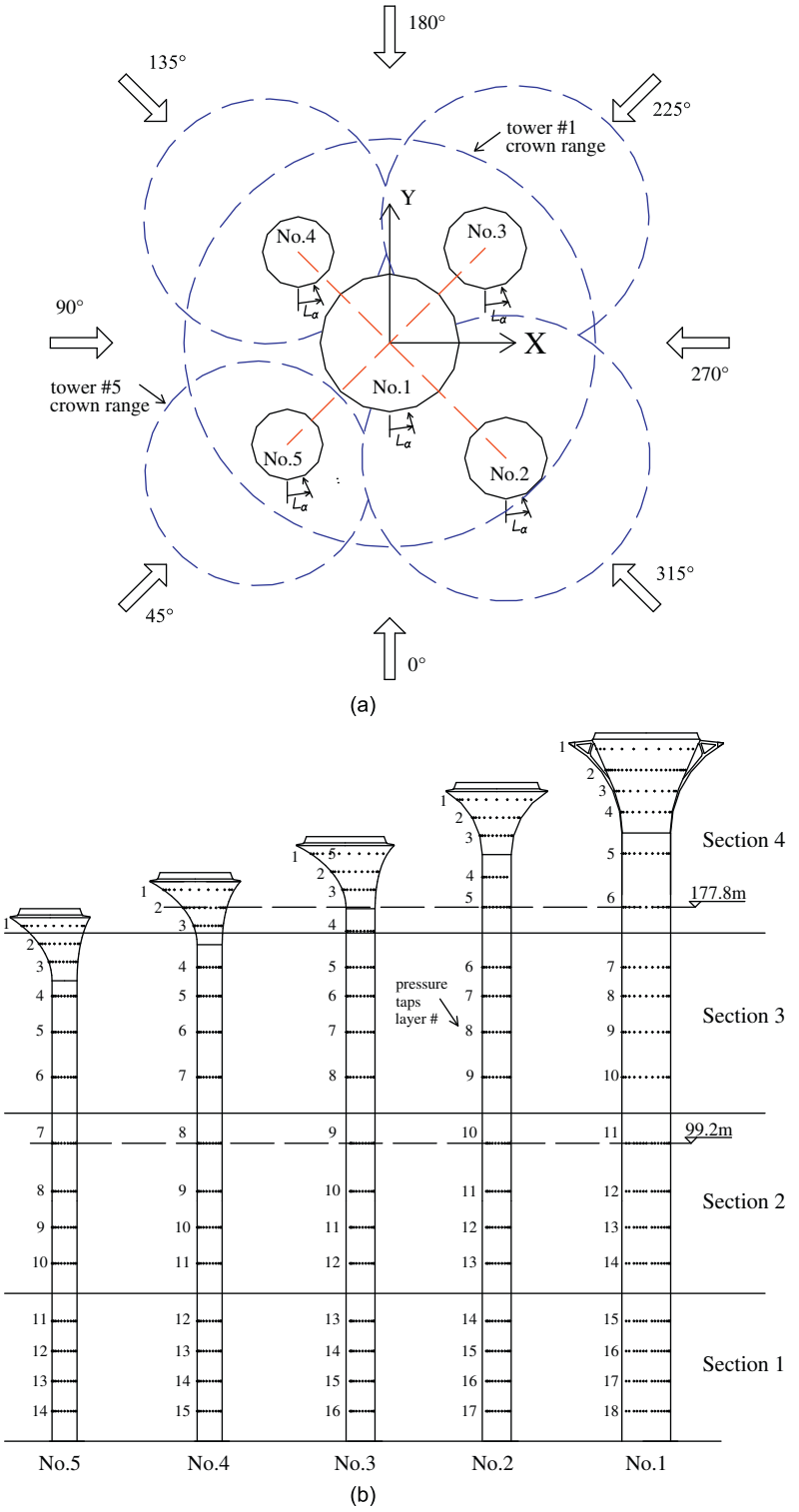

Fig. 1. Layout of group-tower and pressure taps layout: (a) vertical view and (b) elevation.

four cylinders in an in-line square configuration using a finite-volume method. The relations between the flow pattern transition and the mean and fluctuating pressure characteristics on the cylinder surface, and the mean and fluctuating drag and lift behavior were discussed. The results indicate that successful numerical simulations can reveal important flow characteristics and information which are extremely difficult to obtain experimentally.

In this paper, an actual group-tower model was tested in a wind tunnel to study the distribution characteristics of the wind pressure and wind force on complicated group structures. The group-tower was composed of five separate sub-towers with different diameters and heights. Each sub-tower consisted of a cylindrical body with a top tower crown. The sub-towers labeled as Nos. 1, 2, 3, 4 and 5 were 235.8, 219.3, 201.3, 189.3 and 177.3 m in height, respectively, and were 16.2, 9.6, 9.6, 8.3 and 8.3 m in diameter, respectively. The plane and elevation views of the structure are shown in Fig. 1, which shows that the spacing between the tower bodies was small. The model of the super-lofty structure is clearly unique and complicated from an aerodynamic point of view. This paper studied the distribution characteristics of the wind pressure and wind force and presents the base shear and moment coefficients based on the pressure measurements of the rigid model obtained in wind tunnel tests.

2. Outline of the experiments

2.1. Testing model, testing conditions and treatment of Reynolds number effect

The tests were carried out in the TJ-2 atmospheric boundary wind tunnel at Tongji University. Because all the towers were slender (e.g., the diameter of the smallest tower was 8.3 m, but its height was 177.3 m), it was impossible to measure the pressure on the whole scaled model. Therefore, pressure was measured for sectional models of the group-tower in a uniform, turbulent wind field. The group-tower was divided into four sections along the height: the first section was from 0 to 49.2 m at a 1:70 scale; the second was from 49.2 to 109.2 m at a 1:70 scale; the third was from 109.2 to 169.2 m at a 1:70 scale; and the fourth was the tower crown from 145.8 to 235.8 m at a 1:100 scale. As the tower crown dimension was relatively large, a scale of 1:100 was selected to satisfy the requirement of the blockage ratio. In the sectional models, the relative positions between the sub-towers were invariable. The rigid sectional models of the group-tower are shown in Fig. 2.

There were 1944 pressure taps used for the whole group-tower model arranged in horizontal measurement layers on the sub-towers at different heights. For each tap layer of each sub-tower, the center of the upwind face at the 0° wind direction was set as the origin, and the other points were laid uniformly around each horizontal measurement layer at an interval of 15°, numbered anticlockwise (i.e., there were 24 taps on each horizontal measurement layer). As an exception, on the second (from the top) horizontal measurement layer of the No. 1 sub-tower, the spacing between the pressure taps was much smaller, with 48 taps. The schematic layout of the pressure taps is shown in Fig. 1.

The definition of the azimuth for each tower and the wind direction angle are shown in Fig. 1. The wind direction angle increased clockwise. The wind direction angle was varied by 15°, i.e., the test was performed for 24 wind directions.

Generally, the aerodynamic characteristics of a smooth cylindrical structure will be influenced greatly by the Reynolds number (Simiu and Scanlan, 1996). Because the present model was tested in a wind field with a high turbulence intensity and because serious aerodynamic interferences existed between the sub-towers, the Reynolds number was assumed to have little influence on the tower model (Holmes, 2007). However, to ensure a high Reynolds number, roughness strips were pasted on the model's surface to simulate a high Reynolds number state on the structure. Twenty-four vertical thin strips with cross-sections of 1 mm × 1 mm (for sub-tower No. 1) or 0.5 mm × 0.5 mm (for sub-tower Nos. 2–5) were symmetrically pasted along the circumferential surface of the sub-towers, respectively; these strips met the following requirements for the surface roughness (Simiu and Scanlan, 1996):

$$U*e/v>400 \text{ and } e/D<0.01, \tag{1}$$

where U is the mean wind speed in the test, $v=1.5\times10^{-5}\ \mathrm{m^2/s}$ is the dynamic viscosity of air, e is the width of the roughness strips and D is the diameter of the sub-tower.

2.2. Wind field simulation

Because of the ambient building circumstance around the tower, the open terrain at the tower site was determined and simulated. As there were no other high buildings around, no surrounding buildings were simulated.

Each sectional model test was conducted in a uniform field with a constant mean velocity and turbulence intensity. The uniform turbulence was generated by a turbulence generator with passive grids. The wind velocity was 12.0 m/s. Because there is no clear definition of a distribution of turbulence intensity along the height in the Chinese Code for Loading on Buildings and Structures (GB50009-2001, 2002), the turbulence intensity in the following tests was

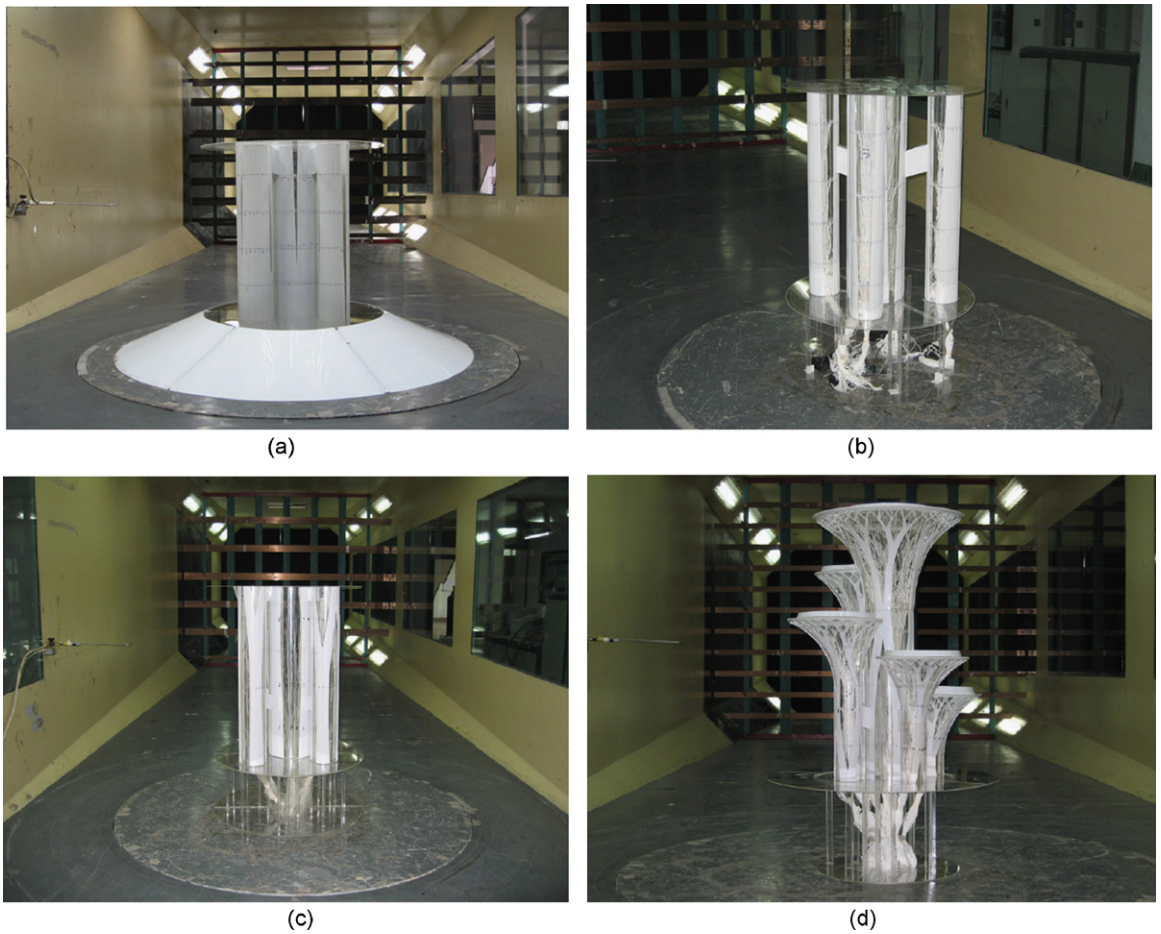

Fig. 2. Rigid sectional models of the group-tower: (a) first section, (b) second section, (c) third section and (d) fourth section.

Table 1
Parameters of the simulated turbulent field with grids.

Numbering of sectional models	Height range (m, height off the ground)	Reference height (m)	Reference turbulence intensity (%)	Simulation turbulence intensity (%)
1	0–49.2	30–40	18–20	18
2	49.2–109.2	70–90	15–16	15
3	109.2–169.2	130–150	13–14	14
4	145.8–235.8	180–200	12	11.5

determined according to the Recommendations for Loads on Buildings by the Architectural Institute of Japan (AIJ, 2004). The simulation results are shown in Table 1.

3. Test results

3.1. Characteristics of wind pressure distribution

The non-dimensional wind pressure coefficient, C_{Pi}, was used to characterize the surface pressure of the building, which is defined as follows:

$$C_{P_i} = (P_i - P_\infty)/(P_0 - P_\infty), \tag{2}$$

where C_{Pi} is the pressure coefficient at i, P_i is the pressure at i and P_0 and P_∞ are the total pressure and the static pressure, respectively. The mean pressure coefficient, $C_{Pi,\mathrm{mean}}$, and the rms pressure coefficient, $C_{Pi,,\mathrm{rms}}$, can then be calculated from C_{Pi}.

3.1.1. Mean pressure coefficients

The characteristics of the pressure distribution will be discussed at the wind directions of 0° and 315°. Because the cross-sections and relative positions of the sub-towers in the height range near 99.2 m have the same shape, the wind flow with those wind directions at that height was relatively stable, and the pressures at that height were selected to be analyzed. Fig. 3 shows the mean pressure coefficients with 0° and 315° wind directions. The towers, Nos. 1–5, denote the five different sub-towers. For each horizontal measurement layer of each sub-tower, 24 taps were spaced uniformly where their positions are defined by the angle, L_α, which increased anticlockwise with the center of the upwind face at the 0° wind direction as the origin (see Fig. 1).

As can be seen from Fig. 3(a), because of the interference, the pressure distribution on each tower was complicated, and the distribution trend and the pressure coefficients were quite different from those on a single circular cylinder. The following summarizes the results. (i) With a 0° wind direction, the maximum positive pressure on the No. 1 sub-tower occurred at the center of the upwind face ($L_\alpha = 0°$) with $C_{P,\mathrm{mean}} = 1.02$. This phenomenon can be accounted for by considering that when wind is passing through the space between the No. 2 and No. 5 sub-towers, the wind speed will increase because of the Venturi effect; thus, the pressure at the stagnation point of the No. 1 sub-tower increased to a value larger than that of a single circular cylinder. (ii) For the pressure distribution on the No. 2 and No. 5 sub-towers, it can be seen that the maximum positive pressure does not occur at the center of the upwind face but at the point when

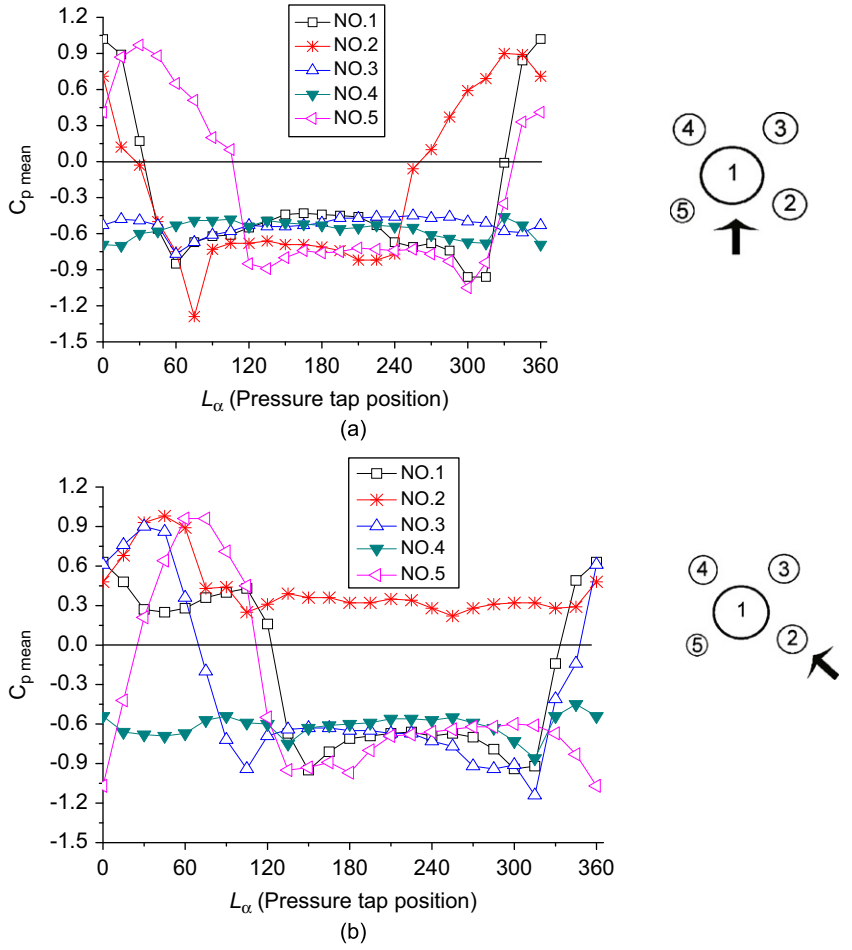

Fig. 3. Mean pressure coefficient on each tap at a height of 99.2 m: (a) 0° wind direction and (b) 315° wind direction.

$L_\alpha = 330^\circ$ with a $C_{P,\text{mean}} = 0.90$ (No. 2 sub-tower) and when $L_\alpha = \sim 30^\circ$, $C_{P,\text{mean}} = 0.97$ (No. 5 sub-tower). The No. 2 and No. 5 sub-towers were positioned almost symmetrically around the No. 1 tower except for the small differences between their diameters and their distance to the No. 1 sub-tower; thus, the pressures on the No. 2 and No. 5 sub-towers were also essentially symmetrical. However, because of the existence of the No. 1, No. 2 and No. 5 sub-towers, when the wind was passing the group-tower, the flow was offset, and the stagnation points on the No. 2 and No. 5 sub-towers were offset inward to 330° and 30°, respectively; accordingly, the mean pressure coefficients of the stagnation points were also different. (iii) Because of the interference of the multi-cylinders and the differences between the two sub-towers, the suction regions of the No. 2 and No. 5 sub-towers were located at $L_\alpha = \sim 30$–255° and $L_\alpha = \sim 120$–330°, respectively. (iv) Moreover, the No. 3 and No. 4 sub-towers were located behind the other three sub-towers, and so the pressures on them were all negative; in this case, from the point of the whole wind force view, the pressures on the No. 3 and No. 4 sub-towers were counteracted partly because the resultant wind forces on those two towers were relatively small.

Fig. 3(b) shows the mean pressure coefficients at the height of 99.2 m with a 315° wind direction. With the 315° wind direction, because of the shielding effect of the No. 2 sub-tower, the upwind pressures on the No. 1 sub-tower were relatively small, with a maximum $C_{P,\text{mean}} = 0.63$. Except for the significant difference between the mean pressures compared to the 0° wind direction, all the pressures on the No. 2 sub-tower were positive, including on the leeward side because of the existence of the No. 1, 3 and 5 sub-towers, though particularly the No. 1 sub-tower. Also at this wind direction, the No. 3 sub-tower was no longer entirely behind the other sub-towers and thus, at a few positions, the mean pressures were positive. With the 315° wind direction, the No. 4 sub-tower was also located behind the other three sub-towers at that wind direction, and so the pressures on the No. 4 sub-tower were all still negative. Furthermore, similar to the above discussion, the pressures on the No. 3 and No. 5 sub-towers were essentially symmetrical, with a smaller offset of the stagnation point compared to that of the No. 3 and No. 5 sub-towers with the 0° wind direction, as now they were in the wake flow of the No. 2 sub-tower.

As a brief summary, the maximum and minimum mean pressure coefficients of each sub-tower at the height of 99.2 m are shown in Table 2. Because of interference effects, the results were quite different with different wind directions.

Because of the complex configurations and the influence of the five tower crowns, the pressure distributions on the upper cylinders near the crowns were somewhat different from those at a height of 99.2 m. Fig. 4 shows the mean pressure coefficients at a height of 177.8 m, which was the height of the No. 5 sub-tower's tip, for the No. 1–No. 4 sub-towers with the 0° and 315° wind directions. With the 0° wind direction, the mean pressure distributions of the No. 1–No. 3 sub-towers were somewhat similar to those at a height of 99.2 m (Fig. 3(a)), whereas for the No. 4 sub-tower, because of the mixed effects of weakening of the shielding function by the No. 5 sub-tower and the complex wake action from the top of the No. 5 sub-tower, the maximum and minimum $C_{P,\text{mean}}$ increased to 0.22 and −1.35, respectively, compared to the $C_{P,\text{mean}}$ at a height of 99.2 m, which ranged from −0.5 to −0.7.

With the 315° wind direction, the wind pressures on the No. 1 sub-tower at $L_\alpha = 330$–360° were influenced by the absence of the No. 5 sub-tower. The maximum $C_{P,\text{mean}}$ on the No. 1 sub-tower occurred at $L_\alpha = 90^\circ$ with the value of 0.90, and $C_{P,\text{mean}}$ was −1.01 at $L_\alpha = 0^\circ$, whereas the maximum $C_{P,\text{mean}}$ occurred at $L_\alpha = 0^\circ$ with value of 0.63 at a height of 99.2 m. Furthermore, the pressure distribution at a height of 177.8 m on the No. 2 sub-tower, which was in front of

Table 2
Comparison of the maximum $C_{P,\text{mean}}$ on the sub-towers at a height of 99.2 m.

Wind direction	Sub-tower #				
	No. 1	No. 2	No. 3	No. 4	No. 5
	Maximum $C_{P,\text{mean}}$ (corresponding L_α)				
0°	1.02 (0°)	0.90 (330°)	−0.45 (255°)	−0.46 (330°)	0.97 (30°)
345°	0.99 (0°)	0.96 (0°)	0.33 (15°)	−0.44 (90°)	0.97 (45°)
330°	0.98 (15°)	0.95 (15°)	0.55 (15°)	−0.20 (90°)	0.99 (60°)
315°	0.63 (0°)	0.98 (45°)	0.90 (30°)	−0.45 (345°)	0.96 (60°)
	Minimal $C_{P,\text{mean}}$ (corresponding L_α)				
0°	−0.96 (300°)	−1.29 (75°)	−0.77 (60°)	−0.70 (15°)	−1.05 (300°)
345°	−0.96 (315°)	−1.06 (75°)	−0.81 (315°)	−0.74 (30°)	−1.17 (315°)
330°	−1.04 (315°)	−0.32 (75°)	−0.85 (315°)	−0.94 (30°)	−1.25 (0°)
315°	−0.95 (150°)	0.22 (255°)	−1.14 (315°)	−0.86 (315°)	−1.07 (0°)

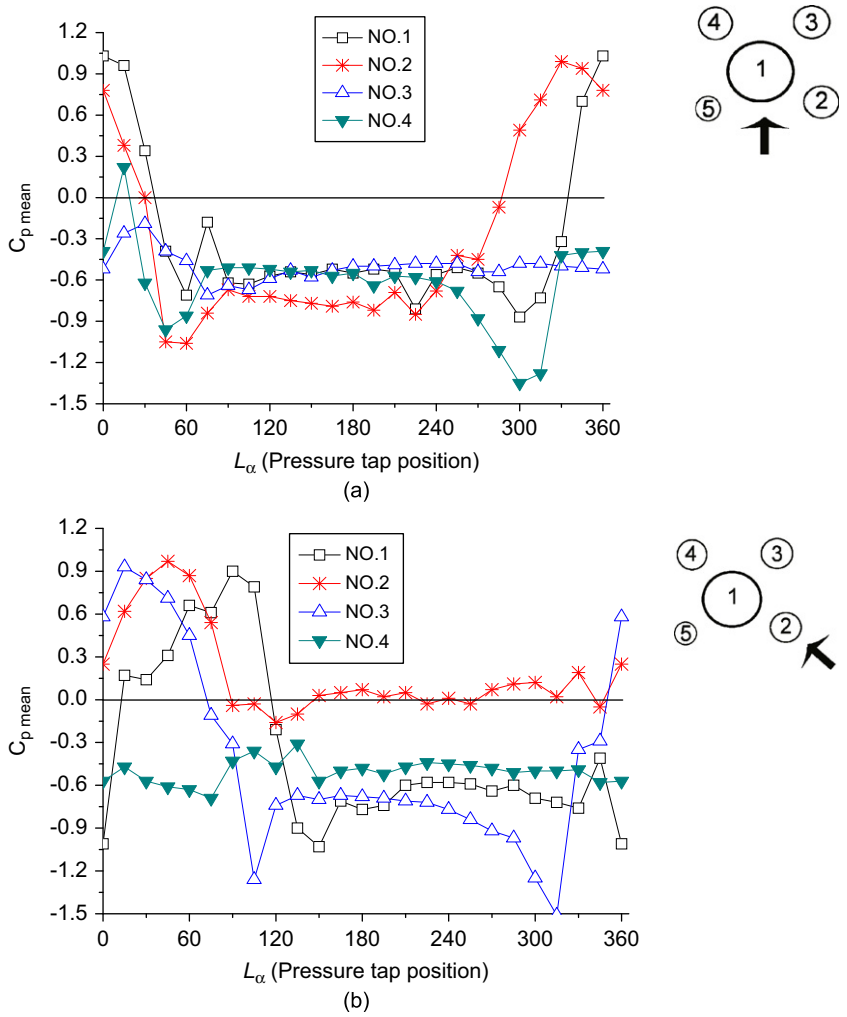

Fig. 4. Mean pressure coefficient on each tap at a height of 177.8 m: (a) 0° wind direction and (b) 315° wind direction.

the No. 5 sub-tower, seemed unaffected by the relative height reduction of the No. 5 sub-tower and also was different from those at a height of 99.2 m because of the flow asymmetry. At a height of 99.2 m, all the pressure coefficients on the No. 2 sub-tower were larger than 0.25, whereas those at 177.8 m were smaller and negative.

3.1.2. Rms pressure coefficients

The rms pressure coefficients on each sub-tower are shown in Fig. 5. Studies (Nishimura and Taniike, 2001; Li and Gu, 2005) have shown two pronounced characteristics of the rms pressure distribution on a single, two-dimensional circular cylinder in uniform flow: first, a minimum upwind rms pressure will exist on the leeward side, and a maximum will exist on the lateral side; second, the distribution of the rms pressure is bilaterally symmetric. As can be seen from Fig. 5, the rms pressure distributions on the present group-tower in the turbulent wind field are clearly different from those on a single tower. The rms pressure coefficients on the No. 1 sub-tower appear relatively symmetrical with the wind direction, whereas those on the other sub-towers have complicated distribution trends. At the upwind pressure taps, when with no interference or with little interference (e.g., the right upwind taps on the No. 2 tower with a 315° wind direction), the rms pressure coefficients show the turbulent effect of the approaching flow, whereas pressures on the lateral surface appear to have a decreasing trend. When the layout of the sub-towers was relatively symmetric, the rms pressures on the symmetrical axis appear to be relatively symmetrical. The rms pressure distribution on a sub-tower in the wake of the other sub-towers was complicated, and a distribution law of the rms pressure coefficients could not be attained. For example, the interference effects on the No. 3 sub-tower from the other sub-towers with wind directions of

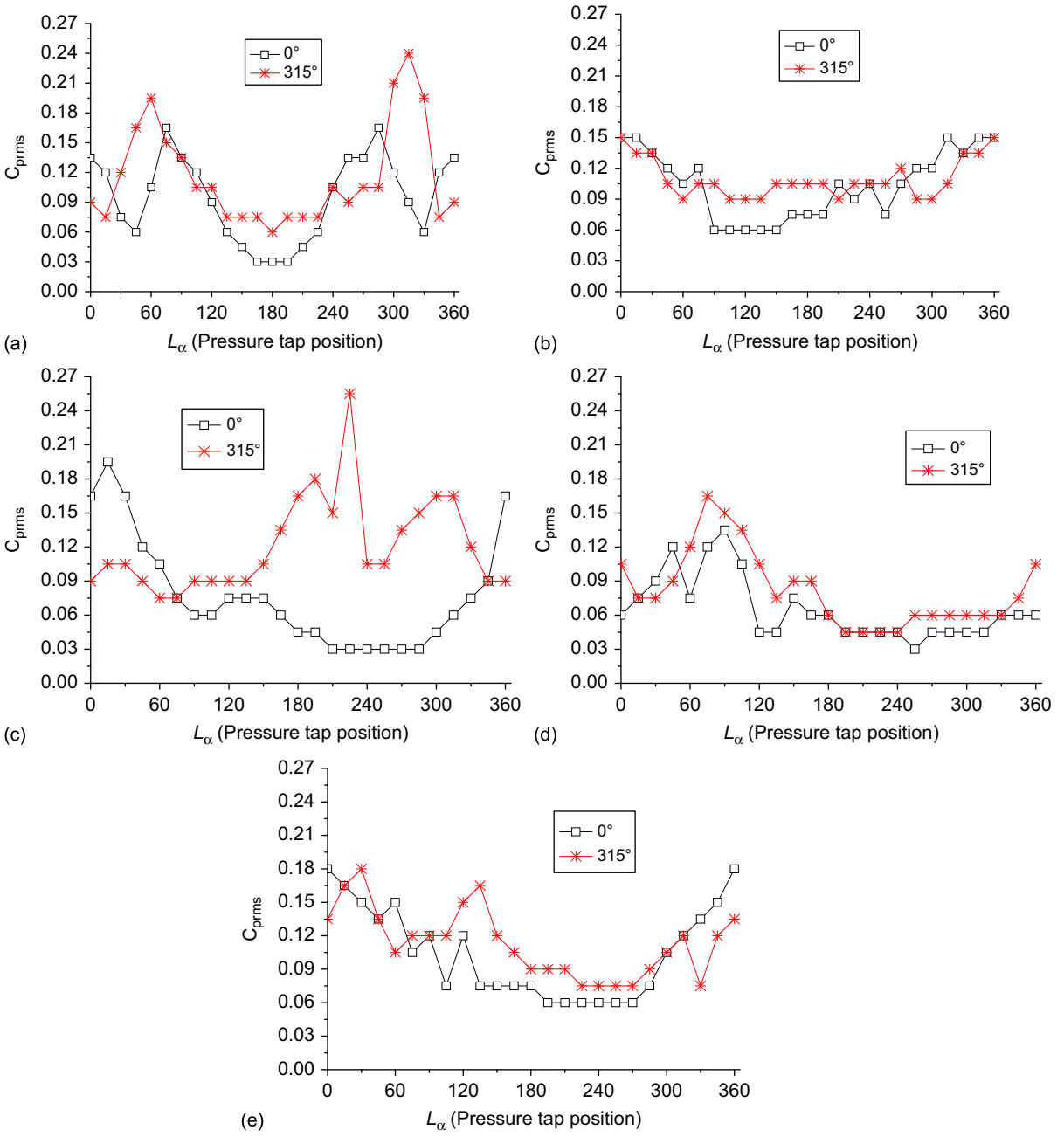

Fig. 5. Rms pressure coefficients: (a) No. 1 sub-tower, (b) No. 2 sub-tower, (c) No. 3 sub-tower, (d) No. 4 sub-tower and (e) No. 5 sub-tower.

0° and 315° were different; thus, the rms pressure distributions were different, whereas at the same two wind directions, the No. 4 sub-tower was always behind the other sub-towers, where the interfered situations were similar, and so its rms pressures were similar.

3.2. *Wind force coefficients*

Using the pressure distribution, the wind force coefficients at each tap layer on each sub-tower with different wind directions were obtained. According to the layout of the pressure taps, there were 80 tap layers on the five sub-towers.

The horizontal mean wind force coefficients of the cross-section along the x and y directions, C_x and C_y, were calculated (the x and y directions are shown in Fig. 1) using Eq. (3):

$$C_x = \sum_{i=1}^{n} C_{pi} A_{ix} \cos(\theta_i)/A, \quad C_y = \sum_{i=1}^{n} C_{pi} A_{iy} \cos(\theta_i)/A, \tag{3}$$

where C_{Pi} is the pressure coefficient at point i, A_{ix} and A_{iy} are the projected area of the affiliated region of the tap along the x and y axes, respectively, θ_i is the obliquity angle of inclination between the normal direction of the tap plane and the horizontal plane. When the diameter of the tower was constant, θ was 0°; for the tower crowns, θ ranged from about 10 to 55°. Also, n is the number of taps of each tap layer; A is the projected area of each circular cylinder along the x and y directions. The mean wind force coefficients ($C_{x,\mathrm{mean}}$, $C_{y,\mathrm{mean}}$) and the rms wind force coefficients ($C_{x,\mathrm{rms}}$, $C_{y,\mathrm{rms}}$) were also obtained.

The mean wind force coefficients on the layers of the sub-towers at two typical wind directions, 0° and 45°, are shown in Fig. 6, where the number of the horizontal coordinate represents the layers on which the wind forces act (see Fig. 1).

As can be seen from Fig. 6, with a 0° wind direction, the No. 1 sub-tower was almost symmetrical with regard to the other sub-towers; thus, the across-wind mean force coefficients, $C_{x,\mathrm{mean}}$, on the No. 1 sub-tower were small; the along-wind mean force coefficient, $C_{y,\mathrm{mean}}$, decreased from about 0.7–0.8 on the top layers to about 0.35 on the base layers. The No. 3 and No. 4 sub-towers were behind the other sub-towers, and their mean wind force coefficients ($C_{x,\mathrm{mean}}$, $C_{y,\mathrm{mean}}$) were therefore smaller, which is consistent with the analysis of the mean pressure coefficient characteristics made before.

When the wind direction was 0°, the No. 1 sub-tower was located in the rear and to the left, and the No. 5 sub-tower was just to the left side of the No. 2 sub-tower; thus, the across-wind mean force coefficients, $C_{x,\mathrm{mean}}$, on the No. 2 sub-tower were positive, i.e., the force increased from left to right because of the flow offsetting. $C_{x,\mathrm{mean}}$ on the No. 5 sub-tower was negative, i.e., the force increased from right to left, which was due to the existence of the No. 1 and No. 2

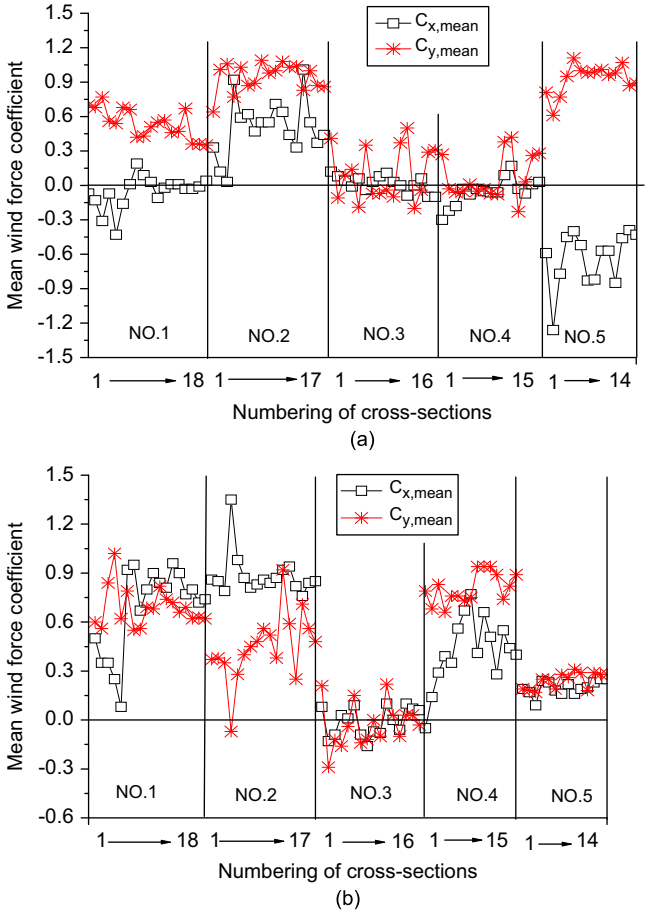

Fig. 6. Mean wind force coefficients on tap layers of the five sub-towers: (a) 0° wind direction and (b) 45° wind direction.

sub-towers. This means that the wind forces on the No. 2 and No. 5 sub-towers along the x direction applied a force outward on those sub-towers, which can also be seen in the analysis of the pressure distributions shown in Fig. 3(a). Moreover, the absolute values of the wind forces in the along- and across-wind directions of the two sub-towers were similar because of their similar shapes and locations relative to the No. 1 sub-tower.

Fig. 6(b) presents the mean wind force coefficients on layers with a 45° wind direction. The No. 3 sub-tower was just behind the other sub-towers at this wind direction; thus, the mean wind forces on the layers of the No. 3 sub-tower were small. The No. 2 sub-tower and the No. 4 sub-tower were almost symmetric about the main tower, i.e., the No. 1 sub-tower, even though their diameters, heights and distances to the main tower differed, the force distributions are similar to some extent. However, the height of the fourth tap layer of the No. 2 sub-tower was slightly higher than the tip of the No. 5 sub-tower (see Fig. 1), and thus was in the wake flow from the tip of the No. 5 sub-tower, and sudden variations of the forces on the fourth tap layer of the No. 2 sub-tower were found. Furthermore, the across-wind forces on the No. 2 and the No. 4 sub-towers both appeared to be directed outward; thus, the wind force projections on the No. 2 sub-tower along the x coordinate were generally larger than those along the y coordinate. For the No. 4 sub-tower, the opposite occurred, wherein the wind force projection was larger along the y coordinate. As for the No. 5 sub-tower, the interference from the other sub-towers was almost symmetrical about this wind direction, the wind forces only varied slightly along the height of the sub-tower, and the projections of the force coefficients in the x and y directions were almost identical.

Fig. 7 shows the rms wind force coefficients ($C_{x,\mathrm{rms}}$, $C_{y,\mathrm{rms}}$) corresponding to the cases in Fig. 6. Generally, the distributions of the rms wind force coefficients along the heights of the five sub-towers with a 0° and 45° wind directions had a similar trend, where the maximum forces generally appeared at the middle of the sub-towers. The reason for this

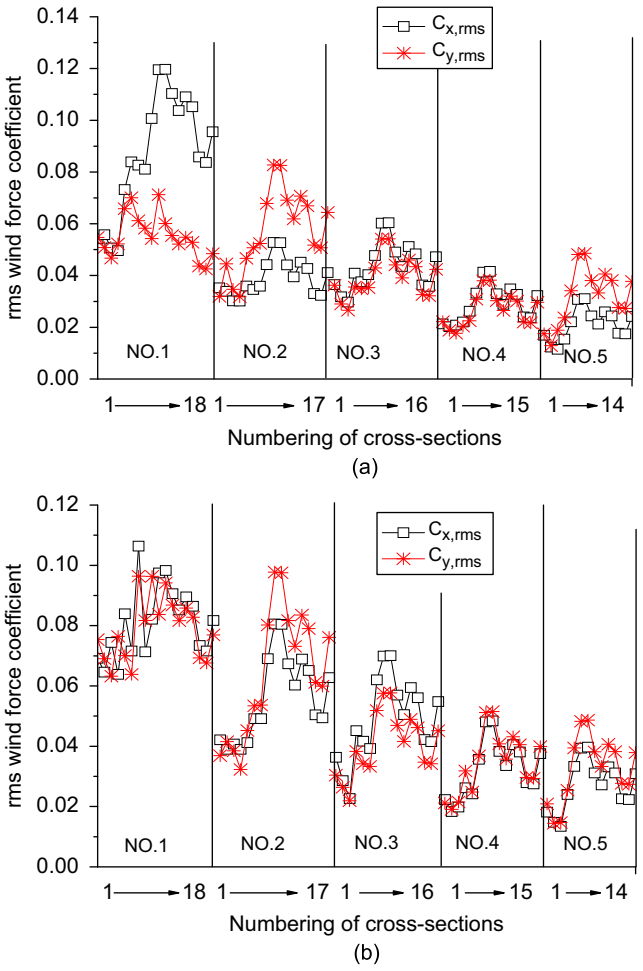

Fig. 7. Rms wind force coefficients on tap layers of the five sub-towers: (a) 0° wind direction and (b) 45° wind direction.

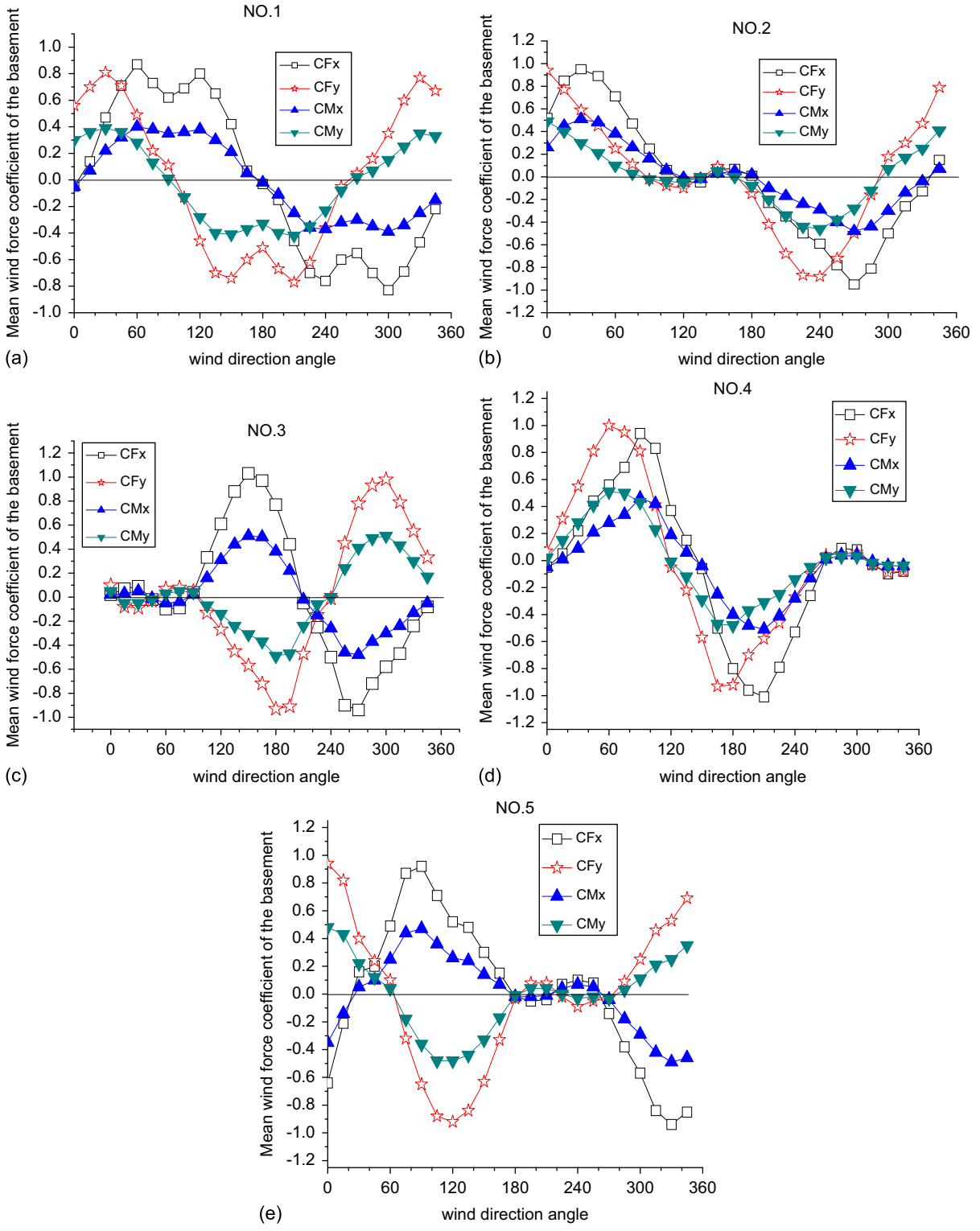

Fig. 8. Mean base wind force coefficients of the five sub-towers: (a) No. 1 sub-tower, (b) No. 2 sub-tower, (c) No. 3 sub-tower, (d) No. 4 sub-tower and (e) No. 5 sub-tower.

phenomenon might be that approximate 2-D flows at the middle of the sub-towers existed, whereas stronger 3-D flows existed at the other parts. It can also be seen that the values of the rms wind force coefficients decreased with an increase in the number of sub-towers, but why this phenomenon occurs is unclear. Moreover, $C_{x,\mathrm{rms}}$ and $C_{y,\mathrm{rms}}$ were almost identical except for the cases of the No. 1 and No. 2 sub-towers with the 0° wind direction. With the 0° wind direction, the rms wind force coefficients on the No. 1 sub-tower in the x direction were larger than those in the y direction (except at the top crown), i.e., the across-wind rms wind force coefficients were larger than those with the along-wind, whereas the rms wind force coefficients on the No. 2 sub-tower acted in the opposite way.

3.3. Mean base shear and moment coefficients

The mean base shear and the moment coefficients on each sub-tower were obtained by Eq. (4):

$$C_F = \sum_{i=1}^{m} C_i A_{ci}/A_s, \quad C_M = \sum_{i=1}^{m} (C_i \times h_i \times A_{ci})/(A_s \times H), \tag{4}$$

where C_F, C_M and C_i denote the mean base shear coefficient, the mean base moment coefficient and the mean wind force coefficient on the ith tap layer ($C_{x,\mathrm{mean}}$ and $C_{y,\mathrm{mean}}$ in Eq. 3), respectively; m denotes the number associated with the tap layer; A_{ci} is the projected area corresponding to C_i; $A_s = \sum_i^m A_{ci}$denotes the total area of the structure; h_i is the height of the ith tap layer off the ground; H is the height of each sub-tower.

The mean base shear and moment coefficients of the five sub-towers along the x and y directions with different wind directions are shown in Fig. 8, where C_{Fx}, C_{Mx}, C_F and C_{My} are the mean base shear and moment coefficients along the x and y directions, respectively.

The No. 2 sub-tower and the No. 4 sub-tower were in opposite locations about the main sub-tower, i.e., the No. 1 sub-tower, and the No. 3 sub-tower and No. 5 sub-tower were also in opposite locations about the main sub-tower. It can be seen that with different wind directions, the variation trend of the mean base shear and moment coefficients of the former group of sub-towers (No. 2 and No. 4 sub-towers) and the latter group of sub-towers (No. 3 and No. 5 sub-towers) were almost the same and appeared similar to sinusoid waves. For the No. 2 and No. 4 sub-towers, the mean base shear and moment coefficients in the x and y coordinate directions varied similarly with wind direction, whereas for the No. 3 and No. 5 sub-towers, the coefficients in the x direction and the in y direction varied with the wind direction in the opposite way. Furthermore, the extreme values of the base shear coefficients were about 1.0 and -1.0 and about two times larger than the extreme values of the base moment coefficients. The results of mean base shear and moment coefficients could be used to decide the most unfavorable wind direction for a structural design.

Unfortunately, the fluctuating base shear and moment coefficients of the sub-towers are not discussed in this paper because the wind tunnel tests on the sectional models were carried out separately as mentioned above. Accordingly, the correlation characteristics between the forces acting on the sectional models cannot be known, and the fluctuating base shear and moment coefficients cannot be computed precisely based on the results from the sectional models.

4. Concluding remarks

The characteristics of the wind pressures and wind forces on five separate sub-towers of a group-tower were investigated experimentally. Significant mutual aerodynamic interference effects among the sub-towers existed; thus, complicated wind pressure and force distributions were found and discussed. The following conclusions were drawn:

1. Because of the Venturi effect caused by two sub-towers, the maximum mean positive pressure coefficient at the center of the upwind face of the main tower (the No. 1 sub-tower) can exceed 1.0 with a 0° wind direction. For the right and left upwind sub-towers, the stagnation points were offset inward to about 30°, and the mean wind forces on the two towers in the across-wind direction all appear to be directed outward. Moreover, the absolute values of the wind forces in the along and across wind directions of the two sub-towers were similar. For the sub-towers located behind the other towers, the pressures on the sub-towers were all negative, and the resultant integral wind forces on them were relatively small.
2. At the upwind pressure taps, when no interference or little interference existed, the rms pressure coefficients showed a turbulent effect of the approaching flow. Furthermore, the rms pressure coefficients on the No. 1 sub-tower appeared relatively symmetric about the wind direction, whereas those on the other sub-towers had complicated distribution trends. For the rms wind force coefficients, the maximum $C_{x,\mathrm{rms}}$ and $C_{y,\mathrm{rms}}$ on the sub-towers occurred at the middle of the towers (a height of approximately 99.2 m) and decreased gradually sideward.

3. The mean base shear and moment coefficients on the four surrounding sub-towers around the main sub-tower showed two kinds of variation trends with wind direction because of the offsetting flow. Furthermore, the results of mean base shear and moment coefficients could be used to decide the most unfavorable wind direction for a structural design.

Acknowledgements

This research is financially supported by the National Natural Science Foundation of China (90715040, 50708082) and National Technology R&D Program of China (2006BAJ03B04).

References

AIJ, 2004. In: AIJ Recommendations for Loads on Buildings. Architectural Institute of Japan.

Breuera, Peter, Chmielewskib, Tadeusz, 2002. Application of GPS technology to measurements of displacements of high-rise structures due to weak winds. Journal of Wind Engineering and Industrial Aerodynamics 90, 223–230.

GB50009-2001, 2002. In: Chinese Code for Loading on Buildings and Structures. Architectural Industry Press of China, Beijing.

Gu, M., Quan, Y., 2004. Across-wind loads of typical tall buildings. Journal of Wind Engineering and Industrial Aerodynamics 92, 1147–1165.

Gu, Zhifu, Sun, Tianfeng, 1999. On interference between two circular cylinders in staggered arrangement at high subcritical Reynolds numbers. Journal of Wind Engineering and Industrial Aerodynamics 80, 287–309.

Gu, Zhifu, Sun, Tianfeng, 2001. Classifications of flow pattern on three circular cylinders in equilateral-triangular arrangements. Journal of Wind Engineering and Industrial Aerodynamics 89, 553–568.

Holmes, J.D., 2007. In: Wind Loading of Structures 2nd ed. Taylor & Francis.

Katsumuraa, A., Katagirib, J., Marukawab, H., Fujiia, K., 2001. Effects of side ratio on characteristics of across-wind and torsional responses of high-rise buildings. Journal of Wind Engineering and Industrial Aerodynamics 89, 1433–1444.

Kim, Y.M., You, Ki Pyo, 2002. Dynamic responses of a tapered tall building to wind loads. Journal of Wind Engineering and Industrial Aerodynamics 90, 1771–1782.

Li, S.Y., Gu, M., 2005. CFD simulation of the flow around oblique and straight cylinder. Journal of Aerodynamics 23 (2), **222**–227 (in Chinese).

Lam, K., Gong, W.Q., So, R.M.C, 2008. Numerical simulation of cross-flow around four cylinders in an in-line square configuration. Journal of Fluids and Structures 24, 34–57.

Li, H., Sumner, D, 2009. Vortex shedding from two finite circular cylinders in a staggered configuration. Journal of Fluids and Structures 25, 479–505.

Mahon., J., Meskcll., C., 2009. Surface pressure distribution survey in normal triangular tube arrays. Journal of Fluids and Structures 25, 1348–1368.

Masaaki, Ohba, 1998. Experimental study of effects of separation distance between twin high-rise tower models on gaseous diffusion behind the downwind tower model. Journal of Wind Engineering and Industrial Aerodynamics 77&78, 555–566.

Nishimura, H., Taniike, Y., 2001. Aerodynamic characteristics of RMS forces on a circular cylinder. Journal of Wind Engineering and Industrial Aerodynamics 89, 713–723.

Simiu, E., Scanlan, R., 1996. In: Wind Effects on Structures 3rd ed. Wiley, New York.

Sun, T.F., Gu, Z.F., 1995. Interference between wind loading on group of structures. Journal of Wind Engineering and Industrial Aerodynamics 54–55, 213–225.

Xie, Z.N., Gu, M., 2004. Mean interference effects among tall buildings. Engineering Structures 26, 1173–1183.

Xie, Z.N., Gu, M., 2007. Simplified formulas for evaluation of wind-induced interference effects among three tall buildings. Journal of Wind Engineering and Industrial Aerodynamics 95, 31–52.